Anodic Oxide Films on Niobium and Tantalum in Different Aqueous Electrolytes and Their Impedance Characteristics

N. Verma[a,*], K.C. Singh[a], B. Marí[b], M. Mollar[b] and J. Jindal[a]

[a]Department of Chemistry, Maharshi Dayanand University, Rohtak 124001, Haryana, India

[b]Institut de Disseny per la Fabricació Automatitzada, Departament de Física Aplicada,
Universitat Politècnica de València, Camí de Vera s/n, 46022 València, Spain

The anodic oxide films were prepared on the niobium and tantalum in aqueous electrolyte mixtures containing 1 M CH_3COOH + 1 M H_3PO_4 or 1 M CH_3COOH + 1 vol.% HF or 1 M CH_3COOH + 1 M H_3PO_4 + 1 vol.% HF at 30 V for 30 min. The barrier films were obtained on both niobium and tantalum surfaces in all electrolyte mixtures except niobium oxide film formed in 1 M CH_3COOH + 1 vol.% HF which is porous in nature. The anodic oxide films were characterized by FESEM. Also, electrochemical impedance spectroscopy at open-circuit potential on Nb and Ta was applied and obtained data were analyzed by fitting with four different equivalent circuits.

1. Introduction

The anodic oxide film formation on valve metals such as Al, Ta, Nb, and Ti is an exceedingly suitable technique for producing thin oxide films. Niobium and tantalum are well known corrosion resistant materials due to spontaneous formation of anodic oxide film which is passive in nature. The passive thin film blocks the dissolution of the metal in corrosive environment [1]. The researchers have reported that stainless steel coated with niobium increases the corrosion resistance of stainless steel in NaCl solution [2]. The oxide film on Nb and Ta has many technological applications [3–6]. Niobium oxide has been applied in sensing materials [7–9], catalytic processes [10, 11], biocompatible films [12, 13], and in capacitor technology [14, 15]. The use of anodic niobium and tantalum in capacitor technology is due to their high dielectric constant and reduced oxide density. The best volume–capacitance ratio is presently obtained by electrolytic capacitors based on Nb_2O_5 and Ta_2O_5 [16]. Owing to the larger permittivity of the Nb_2O_5 and more natural abundance of Nb, the niobium oxide is considered as substitute of Ta_2O_5 in solid electrolyte tantalum/Ta_2O_5 capacitor [17, 18]. The porous structure on tantalum and niobium is also widely used in optical and electronic devices [19, 20]. Niobium has been also used in piezoelectric materials [21], solar cells [22], etc. Nowadays, Ta_2O_5 and Nb_2O_5 are used as host lattices for rare-earth ion in preparation of luminescent materials [23, 24].

Anodization is well defined process to make oxide film on valve metals like Ta and Nb. The formation of barrier or porous type film depends on the electrolyte composition, temperature, voltage or current density or other anodization parameters. Despite of extensive research on the mechanism and composition of anodic oxide film on Ta and Nb there are fewer publications on porous and non-porous oxide film on Ta and Nb. A highly organized porous niobium oxide film was prepared by anodic oxidation of niobium in H_2SO_4 electrolyte with low concentrations of HF [25]. Porous structure was formed due to partial dissolution of film by reaction of oxide with F^-. The porous structures were also obtained when niobium samples were anodized in 0.001 M Na_2SO_4 + 0.2 wt% HF at 5 V. The microcones of the niobium oxide were reported, prepared by anodizing of niobium in HF electrolyte at standard temperature and pressure [26]. Amorphous niobium oxide made by dc sputtering deposition has been reported [27]. The self order niobium oxide also has been reported, prepared by electrochemical oxidation [25]. Despite of all film forming techniques discussed above and techniques like sol–gel process [28] and chemical vapor deposition [29], the anodic oxidation technique for oxide formation on metals is a less expensive method.

The chemistry and properties of anodic oxide films were highly dependent on the electrolyte used during anodization, therefore in this article we will discuss the formation of anodic oxide film on Nb and Ta in different aqueous electrolytes containing mixture of acetic acid with hydrogen fluoride or with phosphoric acid or their ternary mixture. The goal of this work was to study the morphological characteristics (porous or non-porous) of film formed in the different aqueous electrolyte mixtures and their impedance characteristics.

2. Experimental

Niobium and tantalum foils (99.99% purity Sigma Aldrich) were cut in flag shaped samples for anodic oxidation. The samples were mechanically polished with emery paper up to grade 2400. Prior to the electrochemical treatment the samples were ultrasonically cleaned in acetone and ethanol followed by rinsing in deionised

———————

*corresponding author; e-mail: vermanaveen17@gmail.com

water and finally dried with hot air. Some samples were electropolished in H_2SO_4 + HF + ethylene glycol mixture. The electrochemical cell consisted of a two-electrode system in which large area Pt mesh was used as cathode. The voltage source and measurements of current were operated by Keithley 2400 source meter. The exposed area of the electrode was 1 cm^2. The samples were anodized at constant voltage of 30 V at different electrolyte compositions (1 M CH_3COOH + 1 M H_3PO_4 or 1 M CH_3COOH + 1 vol.% HF or 1 M CH_3COOH + 1 M H_3PO_4 + 1 vol.% HF). Measurement has been performed at room temperature (30 ± 2 °C) in naturally aerated solution. After the anodization treatment the obtained samples were washed with deionized water, ethanol and dried at room temperature.

The electrochemical impedance spectroscopy (EIS) studies were done by PGSTAT (Auto lab potentiostat) at open circuit potentials with three electrode setup with Ag/AgCl used as reference electrode. The electrolyte used was 1 M KCl solution in all impedance measurements. The module was controlled by Nova software. The frequency range of the impedance measurements was 0.1 Hz–100 kHz at ac amplitude of 10 mV. The fitting of the data to equivalent circuits was performed using Zview software. The surface morphology of the film was investigated by FESEM Ultra 55(Zeiss Oxford Instruments).

3. Results and discussion

3.1. Anodic films on niobium

3.1.1. Morphological analysis

Figures 1 and 2 show the field emission scanning electron microscopy (FESEM) images of the niobium oxide film formed on niobium in different aqueous electrolyte mixtures at 30 V for 30 min. The porous structures of niobium oxide were obtained after the anodic oxidation process proceeded in the aqueous electrolyte mixture of composition 1 M CH_3COOH + 1 vol.% HF (Fig. 1). In other electrolyte mixtures with composition 1 M CH_3COOH + 1 M H_3PO_4 or 1 M CH_3COOH + 1 M H_3PO_4 + 1 vol.% HF barrier films were formed. Previously reported works [25, 30] reveal that the presence of F^- in the electrolyte mixture causes the dissolution of oxide film on metals like niobium and tantalum which triggers pore formation. But despite the presence of F^- ion, the niobium samples anodically oxidized in 1 M CH_3COOH + 1 M H_3PO_4 + 1 vol.% HF mixtures do not show porous behavior. It means that pore formations were retarded in the presence of phosphoric acid. It may be due to the potential threshold for formation of pores shifts towards more anodic direction, caused by formation of thicker protective oxide films by phosphate or decrease in electrochemical reaction areas by F^- due to competitive adsorption of F^- and PO_4^{3-} on the surface of niobium [31].

Figure 1a shows the porous niobium oxide film formed on the niobium samples in 1 M CH_3COOH + 1 vol.% HF.

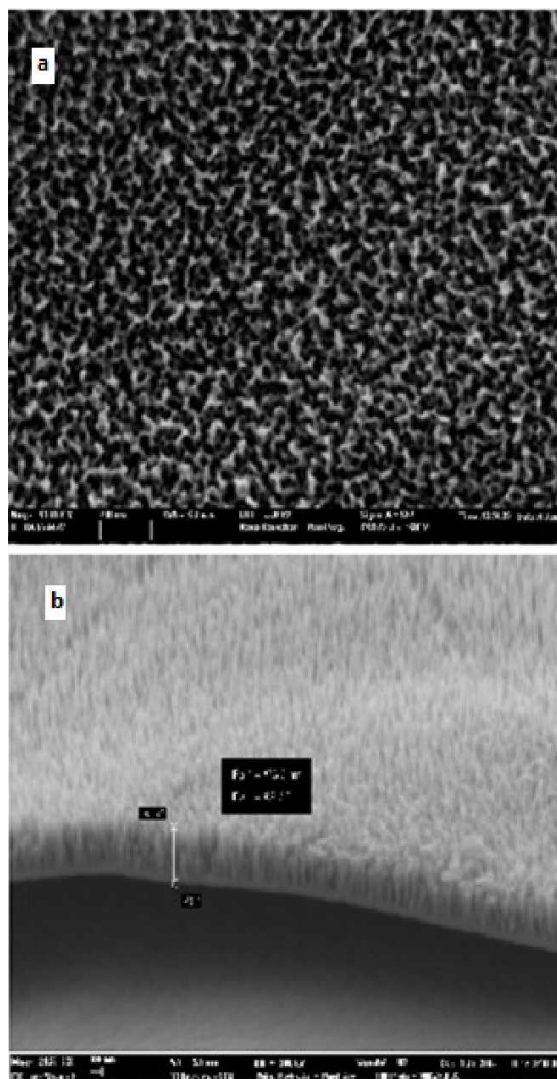Fig. 1. FESEM images of niobium oxide in 1M CH_3COOH + 1 vol % HF for 30 minutes at 30 V: (a) surface view (b) cross section view.

The niobium oxide film has well defined pore distribution with nanosized pores, ranging from 15 nm to 25 nm. The pores were spread out on whole of the surface. The pore density found for this porous template is 2.2×10^{14} m^{-2}. For the obtaining of information about depth distribution, the FESEM cross-section was investigated for porous niobium oxide formed in 1 M CH_3COOH + 1 vol.% HF at 30 V for 30 min shown in Fig. 1b. The FESEM cross-section images show that niobium oxide film consist of two parts, the inner part adjacent to the metallic niobium surface having thickness about 40–50 nm which is highly compact barrier film and pores were oriented vertically against the surface giving total thickness of film about 375 nm. The aspect ratio of layer is found nearly 20. Similar behavior was observed in the reported work at 20 V anodization in the mixture of 1 M H_2SO_4 + 1 wt% HF [25]. The formation of compact layer of 40–50 nm confirms the assumption

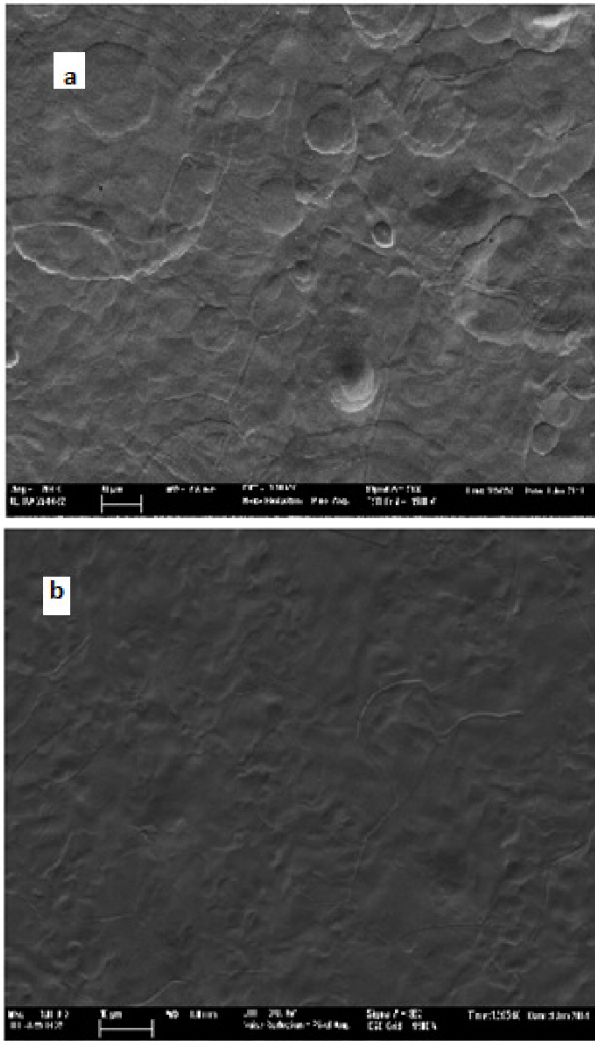Fig. 2. FESEM images of niobium oxide film formed for 30 minutes at 30 V in 1M CH$_3$COOH + 1M H$_3$PO$_4$ (a); 1M CH$_3$COOH + 1M H$_3$PO$_4$ + 1 vol % HF (b).

that pores grow in high field. The porous structure in the cross-section shows parallel pores with homogeneous porosity.

Anodizing in different electrolyte mixtures, the oxide film shows different color. This production of color is based on the phenomenon known as optical interference of light [32, 33]. The samples anodized in 1 M CH$_3$COOH + 1 M H$_3$PO$_4$, 1 M CH$_3$COOH + 1 vol.% HF, and 1 M CH$_3$COOH + 1 M H$_3$PO$_4$ + 1 vol.% HF mixtures show light green, yellow and metallic gray in color, respectively.

3.1.2. Impedance spectroscopy analysis

The electrochemical impedance spectroscopy at open-circuit potential was studied on the films formed on niobium metal in aqueous electrolyte with different compositions. The impedance measurements of film formed in different electrolyte mixtures are shown in Fig. 3. The points in this figure are experimental measurements and lines are fitted curves with equivalent circuits (shown in Fig. 4). The obtained impedance experimental data for film formed in 1 M CH$_3$COOH + 1 M H$_3$PO$_4$ is well fitted with the Randles electrical circuit, which is one of the most common circuits. The circuit includes an uncompensated solution resistance (R_{sol}), a double layer capacitor or constant phase element (CPE) and a polarization resistance (R_p). This is the starting point for other complex models. In our work we have used CPE to fit the impedance of passive metal electrode. The meaning of CPE is based on the oxide film showing the behavior of non-ideal capacitor. The capacitance C_y is related to the thickness of the oxide film d by Eq. (1):

$$C_y = \varepsilon_0 \varepsilon A/d, \qquad (1)$$

where ε is the dielectric constant of film and ε_0 is the permittivity of the free space, A is the surface area. Capacitance data were obtained from fitting parameters by equivalent model shown in Fig. 4a and the thickness of the film is calculated and was found as 64.6 nm. This model is generally applied for the barrier oxide films on the metals. The evaluated impedance parameters from the fitted model are given in Table I.

TABLE I

Different parameters for niobium oxide formed from 1M CH$_3$COOH + 1M H$_3$PO$_4$ obtained from fitting the impedance data with equivalent circuit.

electrolyte	R_{sol} [Ω]	CPE [F]	R_p [Ω]
1M CH$_3$COOH + 1M H$_3$PO$_4$	3.31	0.57×10^{-6}	1.57×10^6

TABLE II

Different parameters for niobium oxside formed from 1M CH$_3$COOH + 1 vol.% % HF obtained from fitting the impedance data with equivalent circuit.

anodizing electrolyte	R_1 [Ω]	R_2 [Ω]	R_3 [Ω]	CPE_1 [F]	CPE_2 [F]
CH$_3$COOH + 1 vol.% HF	4.9	52.25	15910	0.135×10^{-6}	0.055×10^{-6}

The film formed on niobium metal in 1 M CH$_3$COOH + 1 vol.% HF has different types of impedance characteristics than film formed in 1 M CH$_3$COOH + 1 M H$_3$PO$_4$. Figure 4b shows the equivalent circuit to model the anodic oxide film on niobium formed in 1 M CH$_3$COOH + 1 vol.% HF. This circuit was normally used for fitting porous layer. The circuit consists of two RC circuits and one resistance
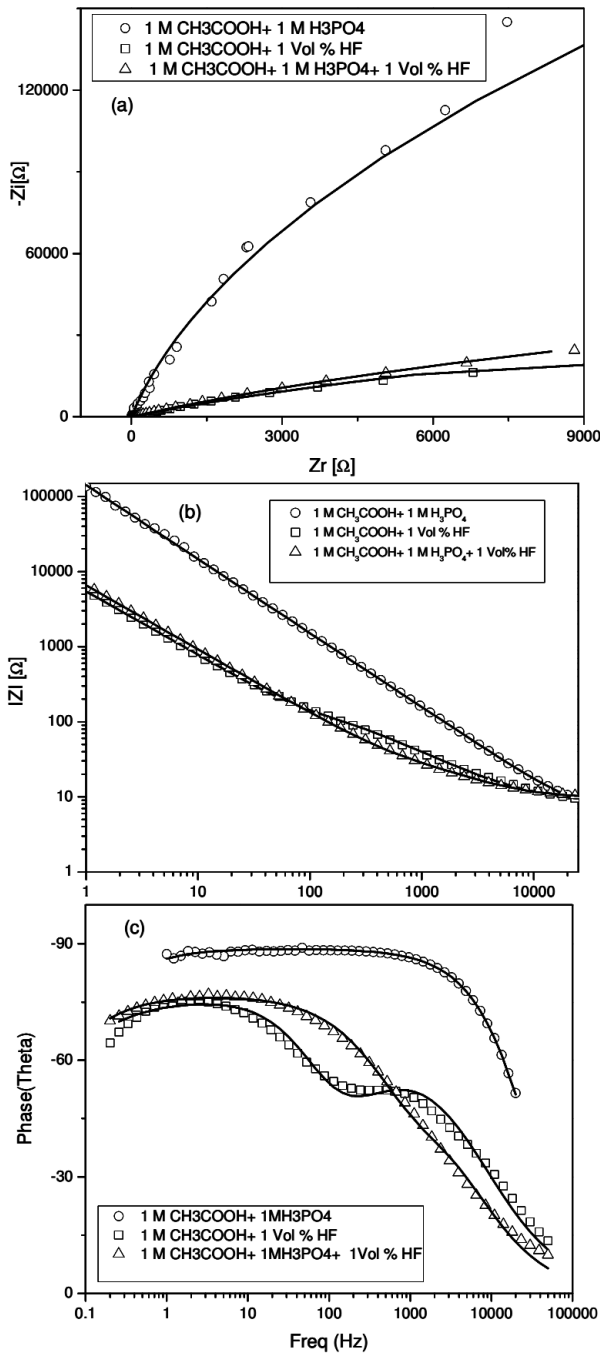
Fig. 3. Electrochemical impedance plots obtained for niobium oxide films at the open-circuit potential from all three electrolytes: Nyquist (a); Bode impedance modulus (b); Bode phase angle (c).
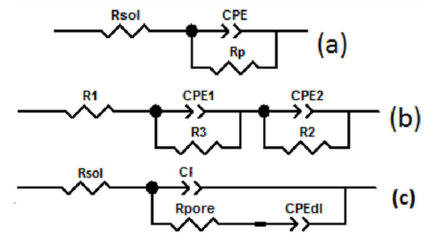

Fig. 4. Equivalent circuits fitted to experimental EIS data of anodic oxide film on niobium.
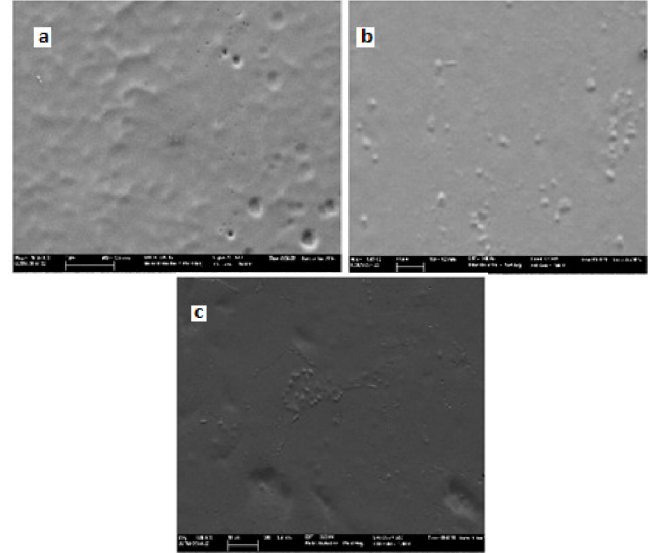

Fig. 5. FESEM images of tantalum oxide formed in 1M CH_3COOH + 1M H_3PO_4 (a); 1M CH_3COOH + 1 vol % HF (b); 1M CH_3COOH + 1M H_3PO_4 + 1 vol% HF (c) for 30 minutes at 30 V.

$R1$; all these are connected in series. $R3CPE1$ circuit corresponds to barrier layer in contact with niobium metal and $R2CPE2$ with porous layer formed. The CPE is frequently used instead of pure capacitance to describe interfacial dielectric properties due to presence of variation in heterogeneities in barrier and porous layer. The resistance R_{sol} is the resistance associated with solution. The resistance R2 of the porous layer is

very low due to ingress of the electrolyte into the pores. The incorporation of the second (R2CPE2) combination is necessary to improve the accurate estimation of EIS data. All the values obtained from modeling by this equivalent circuit are given in Table II.

The experimental impedance data were fitted with Zview software and the good agreement was observed between the experimental results and simulated curves proving that the proposed model is appropriate. The porous nature of the film is also confirmed by the FE-SEM image shown in Fig. 2.

The impedance characteristic of the niobium oxide film formed in 1 M CH_3COOH + 1 M H_3PO_4 + 1 vol.% HF aqueous solution was modeled with an equivalent circuit (Fig. 4c) showing a coated substrate model where R_{sol} is the resistance solution i.e. ohmic drop across the electrolyte. This circuit has been proposed to describe the protective coatings on the metal substrates [27, 34]. In the circuit, capacitance of the perfect coating is represented by C_1 and CPE_{dl} for typical double layer capacitance and ion conduction path in the film due to presence of pores or defects represented by R_{pore} (equivalent circuit is shown in Fig. 4c). The percentage error was typically less than 2.5% on the CPE el-
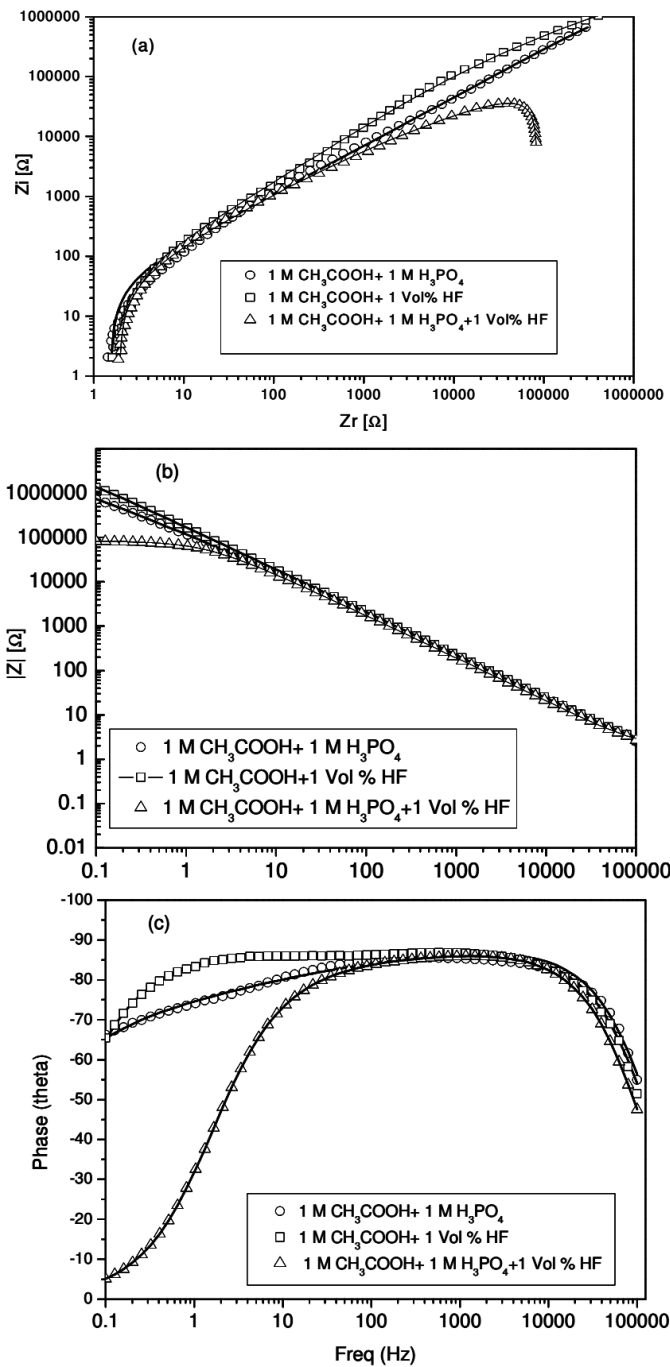
Fig. 6. Electrochemical impedance plots obtained for tantalum oxide films at the open-circuit potential from all three electrolytes: Nyquist (a); Bode impedance modulus (b); Bode phase angle (c).
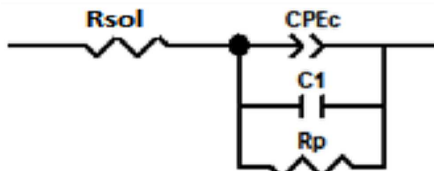

Fig. 7. Equivalent circuit fitted to experimental EIS data of anodic oxide film on tantalum.

ement and 5 to 10% on other circuit elements. All the values of parameters obtained from modeling by this equivalent circuit are given in Table III. In the impedance data plots (Fig. 3a,b) it can be observed that the film formed in 1 M CH_3COOH + 1 M H_3PO_4 shows more compact behavior than film formed in 1 M CH_3COOH + 1 M H_3PO_4 + 1 vol.% HF or 1 M CH_3COOH + 1 vol.% HF electrolyte mixture. This film has shown high impedance value and in the Bode phase plot (Fig. 3c); thus, a phase angle of $-90°$ was observed in frequency range from 1 Hz to 10^3 Hz. The Bode plot for film formed in 1 M CH_3COOH + 1 vol.% HF shows that the impedance spectra consist of two time constants at low and intermediate frequency range (Fig. 3c) showing the porous nature of the film. The Bode impedance modulus plot reveals the lower magnitude of $|Z|$ in case of oxide film formed in F^- containing electrolytes. This might be due to slightly more dissolution of niobium oxide in the presence of F^- ions.

3.2. Anodic oxide film on tantalum

3.2.1. Morphological analysis

FESEM analysis (Fig. 5) shows that barrier type oxide films were formed on tantalum in all electrolyte compositions (as used in anodic oxidation of niobium) at 30 V for 30 min. There is no pore formation even in the presence of F^- in the electrolyte mixture. In the surface morphology of oxide film formed on tantalum in different aqueous electrolyte no significant difference was observed.

3.2.2. Impedance spectroscopy analysis

The simplest circuit which describes both Nyquist and Bode plots recorded at the open-circuit potential is composed of resistor and constant phase element/capacitor [35]. Such equivalent circuits represent the complex impedance plots (imaginary part of impedance versus real part of impedance) by straight lines. But in our experimental results of impedance measurements, curved plots instead of straight were obtained (Fig. 6a). This suggests that the equivalent circuit should be more complex. The equivalent circuit we have applied to fit the data for tantalum oxide film is shown in Fig. 7. This circuit can be derived by a more general case by omission of a capacitor due to space charge layer capacity which is much smaller than that of CPE [36, 37]. All the elements of applied circuit were found to behave in a constant manner. The series resistance R_{sol} is the electrolyte resistance and comes out to be 1.4 ± 0.5 Ω in all samples. The CPE is constant phase element associated with disorder either in electrode structure or in diffusion dynamics. The CPE behavior may also arise due to incorporation of species in outer layer of oxide film which creates localized states in the forbidden band and induces a dispersion of the intrinsic polarization properties of the anodic oxide [38, 39]. C1 is the space charge layer capacitance. There is good agreement between experimental data and fitted data by this equivalent circuit in whole frequency range from 10^{-1} to 10^5 Hz. High values of Rp are obtained, representing the resistance of

the dielectric anodic oxide film. The magnitude of Rp is higher in film formed in 1 M CH_3COOH + H_3PO_4 mixture as compared to the same composition with presence of fluoride ion. This may be due to appearance of some flaws in the film in the presence of fluoride ions. The magnitude of Rp is in good agreement with the nature of the film which behaves as a wide gap semiconductor or even insulator [40]. The measured spectra show that the impedance behavior represents the passive oxide layer characteristics in which capacitive response is illustrated by phase angle above $-80°$ over a wide frequency range. Figure 6c shows that there is no significant differences in the spectra of tantalum oxide film formed in CH_3COOH + H_3PO_4 and CH_3COOH + 1 vol.% HF but film formed in CH_3COOH + H_3PO_4+1 vol.% HF is slightly different which shows a phase decline at lower frequencies. The film formed in CH_3COOH + 1 vol.% HF has highest value of capacitance. This may be due to some decrease in thickness caused due to etching in the presence of F^-. As thickness and capacitance has reciprocate relation so these oxide films have higher capacitance. The obtained parameters by fitting equivalent circuits to the experimental data are given in Table IV.

TABLE III

Different parameters for niobium oxide formed from 1M CH_3COOH + 1M H_3PO_4 + 1 vol.% HF obtained from fitting the impedance data with equivalent circuit.

electrolyte composition	R_{sol} [Ω]	C_1 [F]	CPE_{dl} [F]	R_{pore} [Ω]
1M CH_3COOH + 1M H_3PO_4 + 1 vol.% HF	4.98	1.72×10^{-6}	2.9×10^{-5}	9.39

TABLE IV

Different parameters for tantalum oxide formed from all three electrolytes obtained from fitting the impedance data with equivalent circuit.

electrolyte mixture	R_{sol} [Ω]	CPE_c [F]	C_1 [F]	R_p [Ω]
1M CH_3COOH + 1M H_3PO_4	0.77	0.64×10^{-6}	3.20×10^{-7}	3.52×10^6
1M CH_3COOH + 1 vol.% HF	0.94	3.25×10^{-5}	0.57×10^{-6}	3.66×10^5
1M CH_3COOH + 1M H_3PO_4 + 1 vol.% HF	0.96	4.90×10^{-7}	0.44×10^{-7}	42056

4. Conclusions

In investigations regarding the effect of electrolyte on the formation of oxide film on niobium we found that in the mixtures of 1 M CH_3COOH + 1 M H_3PO_4 or 1 M CH_3COOH + 1 M H_3PO_4 + 1 vol.% HF non-porous compact film was obtained but in 1 M CH_3COOH + 1 vol.% HF mixture we have noticed the porous film having aspect ratio nearly 20 and thickness 375 nm. It means that pore formation was retarded by phosphoric acid at the applied experimental conditions. In the case of formation of oxide film on tantalum we found that in all the electrolyte compositions i.e. 1 M CH_3COOH + 1 M H_3PO_4 or 1 M CH_3COOH + 1 M H_3PO_4 + 1 vol.% HF or 1 M CH_3COOH + 1 vol.% HF mixtures the non-porous films were formed. The impedance data of the oxide films on niobium and tantalum predict the semiconductor or insulator behavior with wide band gap of the oxide film.

Acknowledgments

References

[1] S. Hornkjol, *Electrochim. Acta* **36**, 1443 (1991).

[2] J.H. Hsieh, R. Lee, R.A. Erck, G.R. Fenske, Y.Y. Su, M. Marek, R.F. Hochman, *Surf. Coat. Technol.* **49**, 83 (1991).

[3] T. Balaji, R. Govindaiah, M.K. Sharma, Y. Purushotham, A. Kumar, T.L. Prakash, *Mater. Lett.* **56**, 560 (2002).

[4] J.E. Yoo, J. Choi, *Electrochem. Commun.* **13**, 298 (2011).

[5] H. Stormer, A. Weber, V. Fischer, E.I. Tiffee, D. Gerthsen, *J. Eur. Ceram. Soc.* **29**, 1743 (2009).

[6] S.V.J. Chandra, S. Uthanna, G.M. Rao, *Appl. Surf. Sci.* **254**, 1953 (2008).

[7] S. Rho, D. Jahng, J.H. Lim, J. Choi, J.H. Chang, S.C. Lee, K.J. Kim, *Biosens. Bioelectron.* **23**, 852 (2008).

[8] T. Tamai, M. Haneda, T. Fujitani, H. Hamada, *Catal. Commun.* **8**, 885 (2007).

[9] R. Binions, C.J. Carmalt, I.P. Parkin, *Meas. Sci. Technol.* **18**, 190 (2007).

[10] T. Shishido, T. Miyatake, K. Teramura, Y. Hitomi, H. Yamashita, T. Tanaka, *J. Phys. Chem.* **C113**, 18713 (2009).

[11] A.G.S. Prado, L.B. Bolzon, C.P. Pedroso, A.O. Moura, L.L. Costa, *Appl. Catal. B Environ.* **82**, 219 (2008).

[12] M.T. Tanvir, Y. Aoki, H. Habazaki, *Appl. Surf. Sci.* **255**, 8383 (2009).

[13] A. Ochsenbein, F. Chai, S. Winter, M. Traisnel, J. Breme, H.F. Hildebrand, *Acta Biomater.* **4**, 1506 (2008).

[14] K. Cho, J. Lee, J.S. Lim, H. Lim, J. Lee, S. Park, C.Y. Yoo, S.T. Kim, U.I. Chung, J.T. Moon, *Microelectron. Eng.* **80**, 317 (2005).

[15] J. Li, D. Yi, J. Wen, H. Zhong, H. Liu, *Trans. Nonferrous Met. Soc. China* **16**, 848 (2006).

[16] A. Michaelis, *Advanced Ceramic Oxides for Electronics*, Fraunhofer IRB Verlag, Stuttgart 2006.

[17] J.S. Yoon, S.W. Cho, Y.S. Kim, B. Kim, *Met. Mater. Int.* **15**, 405 (2009).

[18] H. Habazaki, T. Ogasawara, H. Konno, K. Shimizu, S. Nagata, K. Asami, K. Takayama, P. Skeldon, G.E. Thompson, *J. Electrochem. Soc.* **153**, B173 (2006).

[19] R.L. Aagard, *Appl. Phys. Lett.* **27**, 605 (1975).

[20] B. Ohtani, K. Iwai, S. Nishimoto, T. Inui, *J. Electrochem. Soc.* **141**, 2439 (1994).

[21] X. Cheng, Q. Gou, J. Wu, X. Wang, B. Zhang, D. Xiao, J. Zhu, X. Wang, X. Lou, *Ceram. Int.* **40**, 5771 (2014).

[22] M. Mazur, M. Szymanska, D. Kaczmarek, M. Kalisz, D. Wojcieszak, J. Domaradzki, F. Placido, *Appl. Surf. Sci.* **301**, 63 (2014).

[23] D.L. Zhang, P.R. Hua, Y.M. Cui, C.H. Chen, E.Y.B. Pun, *J. Lumin.* **127**, 453 (2007).

[24] S.K. Mahesh, P.P. Rao, T.L. Francis, V.R. Reshmi, P. Koshy, *Mater. Lett.* **120**, 115 (2014).

[25] I. Sieber, H. Hildebrand, A. Friedrich, P. Schmuki, *Electrochem. Commun.* **7**, 97 (2005).

[26] R.L. Karlinsey, *Electrochem. Commun.* **7**, 1190 (2005).

[27] G. Ramirez, S.E. Rodil, S. Muhl, D.T. Ortega, J.J. Olaya, M. Rivera, E. Camps, L.E. Alarcon, *J. Non-Cryst. Solids* **356**, 2714 (2010).

[28] N. Ozer, M.D. Rubin, C.M. Lampert, *Solid En. Mater. Sol. Cells* **40**, 285 (1996).

[29] J.P. Masse, H. Szymanowski, O. Zabeida, A. Amassian, J.E.K. Sapieha, L. Martinu, *Thin Solid Films* **515**, 1674 (2006).

[30] B. Tzvetkov, M. Bojinov, A. Girginov, *J. Solid State Electrochem.* **13**, 1215 (2009).

[31] J. Choi, J.H. Lim, S.C. Lee, J.H. Chang, K.J. Kim, M.A. Cho, *Electrochim. Acta* **51**, 5502 (2006).

[32] M.B.J.G. Freitas, L.O.S. Bulhoes, *J. Appl. Electrochem.* **27**, 612 (1997).

[33] N. Magnussen, L. Quinones, D.C. Dufner, D.L. Cocke, E.A. Schweikert, B.K. Patnaik, C.V.B. Leite, G.B. Baptista, *Chem. Mater.* **1**, 220 (1989).

[34] C. Liu, Q. Bi, A. Leyland, A. Matthews, *Corros. Sci.* **45**, 1257 (2003).

[35] P. Pasierb, S. Komornicki, R. Gajerski, S. Kozinski, P. Tomczyk, M. Rekas, *J. Electroceram.* **8**, 49 (2002).

[36] A. Wahl, M. Ulmann, A. Carroy, B. Jermann, M. Dolata, P. Kedzierzawski, C. Chatelain, A. Monnier, J. Augustynski, *J. Electroanal. Chem.* **396**, 41 (1995).

[37] M. Radecka, M. Wierzbicka, M. Rekas, *Physica B Condens. Matter* **351**, 121 (2004).

[38] Q. Lu, S. Mato, P. Skeldon, G.E. Thompson, D. Masheder, *Thin Solid Films* **429**, 238 (2003).

[39] O. Kerrec, D. Devilliers, H. Groult, M. Chemla, *Electrochim. Acta* **40**, 719 (1995).

[40] J.W. Schultze, V.A. Macagno, *Electrochim. Acta* **31**, 355 (1986).